The regulation of cell cycle exit during *Caenorhabditis elegans* vulva formation

Master thesis Veterinary Medicine at the
Developmental Biology division of Utrecht University
Daily supervisor: Dr. V.C. Portegijs
Date: October 19, 2020

Name: Jolanda Nieuwland
Student number: 5711568
E-mail: j.nieuwland2@students.uu.nl

Abstract

Careful coordination of the division, growth and differentiation of cells is important for the development of a multicellular organism. When factors that normally ensure cell cycle exit are disturbed, overproliferation of cells can occur. This can lead to a disruption of the tissue organization, which is characteristic for cancer. In this study, *C. elegans* was used to research how cell cycle exit is regulated. Using tissue-specific gene knockout in combination with lineage tracing, genes involved in human cancers and the effect of cell cycle inhibitors were investigated in the vulval epithelium of *C. elegans*. Simultaneous knockout of *cep-1*, *daf-3* and *cki-1* led to a significant increase of vulval cells although the loss of *cep-1* and *daf-3* did not seem to strongly enhance the extra cell division phenotype of *cki-1* knockout animals. Furthermore, the effect of loss of HECT-domain ubiquitin ligase UBR-5 was studied. Loss of *ubr-5* led to a small population of animals in which the cell cycle was not fully arrested, leading to several extra vulval nuclei. This suggests *ubr-5* has a function as an inhibitor of cell cycle exit. Additionally, *swsn-8* leads to overproliferation of vulval nuclei. This is in contrast to the inactivation of *swsn-1*, which predominantly leads to premature cell cycle arrest and only occasionally results in extra cell divisions. A forward genetic screen with *swsn-8* mutants showed aberrant vulvae with apparent extra vulval nuclei, which seems promising to further research. In conclusion, this study indicates multiple factors work together to ensure cell divisions are correctly coordinated during development.

Keywords

Caenorhabditis elegans, Cell Cycle, Cancer, Cell Division, Cell Cycle Regulation, Cyclin-Dependent Kinases, Cyclin-Dependent Kinase Inhibitors, CIP/KIP, Chromatin Remodeling Complexes, SWI/SNF, p53, SMAD4, UBR5, *cep-1*, *daf-3*, *ubr-5*

The development of a multicellular organism from a single fertilized egg involves careful coordination of the division, growth and differentiation of cells.[1, 2] The division of cells, also called proliferation, is important to generate the correct number of cells. When cells reach their terminal fate, they must cease their cell divisions and undergo differentiation. Differentiation is the process in which cells become more specialized. The balance between proliferation and differentiation of cells is regulated in the cell cycle (figure 1).[1-3] In the cell cycle the genetic information stored in the DNA is duplicated and divided between two daughter cells. The DNA replication takes place in the synthesis phase, also known as the S phase. By bundling together the replicated DNA and proteins, two identical sister chromatids are formed. During the mitotic phase, also known as the M phase, the two identical sister chromatids align and separate from each other. The mother cell is cleaved during cytokinesis, which results in two daughter cells that each contain one set of sister chromatids.[4, 5] The S and M phases are separated by gap phases; G1 precedes the S phase and G2 precedes the M phase. Cells do not always immediately replicate again; they can also go through periods of short or extended cell cycle arrest. The time cells spend in this temporary arrest depends on the type of cells. Quiescence (or G0) is a state of temporary cell cycle arrest where cells perform their functions, but do not proliferate. The quiescent stage is reversible as cells may retain the capacity to divide again after receiving mitogenic signals from their surroundings.[4-7] Complex combinations of external signals and cell-intrinsic information are integrated in the cell cycle to control the timing of entering and exiting the major cell cycle phases and the frequency of the cell divisions.[2-4] Specifically, a

combination of positive and negative factors that mainly act during the G1 phase play a central part in the commitment to enter the S phase and therefore in enacting another round of cell division (figure 1). Entry into the S phase is mediated by phosphorylation of factors important for the stability, activation and inhibition of proteins. Furthermore, transcription of genes associated with cell cycle progression is required to enter the S phase.[3-6]

When factors that normally ensure cell cycle exit are disturbed, overproliferation of cells can occur. This can lead to a disruption of the tissue organization, which is characteristic for cancer. For instance, both sustaining proliferative signaling and evading growth suppressors are hallmarks of cancer.[2, 4, 8, 9] Regulation of the cell cycle is central to our understanding of how cell divisions are coordinated during development and why cancer cells continue to cycle.

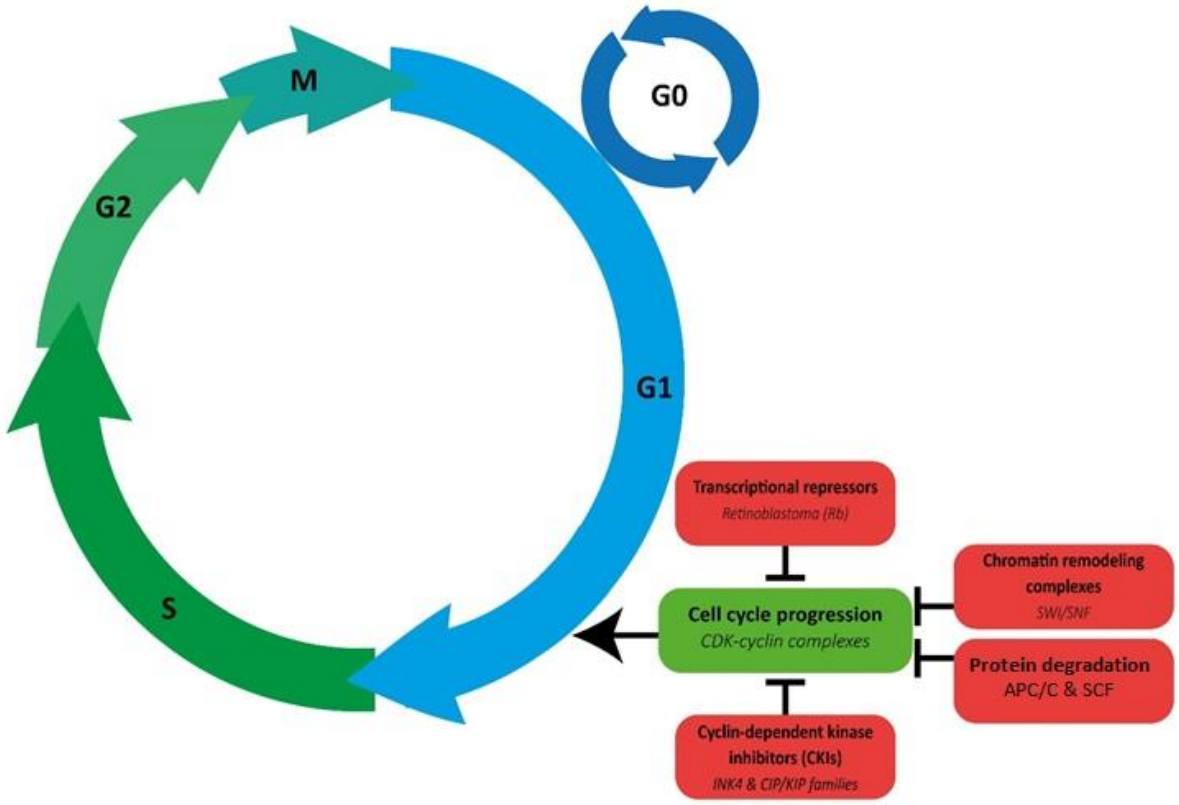

Figure 1. An overview of the cell cycle and the factors that mainly act during the G1 phase, thereby regulating entry into the S phase. The cell cycle consists of the synthesis (S) phase, in which the DNA replication takes place, and the mitosis (M) phase, in which the two identical sister chromatids align and separate from each other. The S and M phases are separated by gap phases; G1 precedes the S phase and G2 precedes the M phase. Quiescence (or G0) is a state of temporary cell cycle arrest where cells perform their functions, but do not proliferate. Complex combinations of external signals and cell-intrinsic information are integrated in the cell cycle to control the timing of entering and exiting the major cell cycle phases and the frequency of the cell divisions. Factors in red indicate inhibitors of S phase entry while the factors in green promote progression of G1 into the S phase.

Amongst the most important positive regulators of cell cycle entry are the cyclin dependent kinase (CDK) – cyclin complexes, which consist of a cyclin subunit and a cyclin dependent kinase.[2, 3, 10] The CDKs can only become enzymatically active when bound to a cyclin. Whereas CDK levels remain relatively stable, the cyclin levels periodically change during different phases of the cell cycle. This helps driving the cyclic assembly and the activation of the CDK-cyclin complexes. Different CDK-cyclin complexes are active in different phases of the cell cycle. For instance, CDK4/6-cyclin D and CDK2-cyclin E complexes promote progression of G1 into the synthesis phase, whereas CDK1-cyclin B drives progression from G2 into the mitotic phase.[2, 3, 10] In addition to the assembly of CDK-cyclin complexes, activation of these complexes in the right phase of the cell cycle requires the removal of inhibitory phosphates and

phosphorylation by CDK activating kinases (CAKs).[11, 12]

Active CDK4/6-cyclin D plays a role in the release of E2F transcription factors, which are important for transcriptional activation of several genes that are critical for progression through the cell cycle. Amongst the activating targets of E2F are Cyclin E and genes involved in apoptosis, mitosis, DNA replication and DNA repair.[13-15] E2F transcription factors are bound by the retinoblastoma tumor suppressor protein (Rb) family of transcriptional co-repressors.[15, 16] The formed Rb-E2F complex blocks the activation of the downstream targets of E2F and silences transcription. Active CDK-cyclin complexes, such as CDK4-cyclin D, phosphorylate Rb, which partially relieves the repression of E2F. This leads to the transcription of, among others, cyclin E, which can associate with CDK2 and further phosphorylate Rb, thereby fully relieving the inhibition of E2F. As a result, full transcription of important cell cycle progression genes occurs. Hence, the assembly of CDK-cyclin complexes drives progression through the cell cycle.[13-17]

In addition to positive regulators, factors that prevent entry into the cell cycle are important in cell cycle regulation. A major mode of regulation is direct inhibition of CDK-cyclin complexes by cyclin-dependent kinase inhibitors (CKIs).[2, 3, 18-20] CKIs oppose progression from the G1 phase to the S phase of the cell cycle. There are two families of CKIs: the INK4 protein family and the CIP/KIP family. CKIs of the INK4 protein family prevent the interaction of CDK4/6 kinases with D-type cyclins by associating with the CDK4/6 kinases. The CKIs of the CIP/KIP family are particularly important for inhibiting CDK2-cyclin E by associating with CDK-cyclin complexes. In humans this family consists of three members, which are $p21^{Cip1}$, $p27^{Kip1}$ and $p57^{Kip2}$.[2, 3, 18-20] These proteins contribute to blocking cell cycle entry and show increased expression in differentiating cells. The differentiation of cells can be initiated by overexpressing cell cycle inhibitors. For example, $p21^{Cip1}$ and $p27^{Kip1}$ overexpression inhibited proliferation and induced differentiation in a variety of tumor cells.[20, 21] A complete loss of the function of CIP/KIP proteins however, is not a common feature of cancers.[18] This indicates the relevance of further understanding how the CKIs inhibit cell cycle entry.

Cell cycle entry is also regulated by targeted protein degradation of positive cell cycle regulators. Proteins are targeted for degradation through the addition of ubiquitin (Ub), which is covalently bound to lysine residues on the target protein.[22-24] This process is called ubiquitination and is mediated by a cascade of enzymes: the ubiquitin-activating enzyme (E1), the ubiquitin-conjugating enzyme (E2) and the ubiquitin ligase (E3). Ubiquitination affects proteins in many ways as it can mark them for degradation via the proteasome (also known as the Ubiquitin-Proteasome System, UPS), but can also alter their cellular location, promote or prevent protein interactions and affect their activity.[22-24] The E3 ubiquitin ligases occupy a key position in the UPS enzymatic cascade as the ligases are largely responsible for determining substrate specificity. The E3 ligases can be categorized in two major classes: the Really Interesting New Gene (RING) family and the homologous to E6AP C terminus (HECT-domain) family.

The RING family E3 ligases mediate the transfer of ubiquitin from E2 to the substrate.[25, 26] Two important families of the multiprotein RING E3 ligases are the anaphase-promoting complex / cyclosome (APC/C) and the Cullin-Ring-Ligase (CRL) complexes, of which the latter includes the Skp1-Cullin-F-box (SCF) complex.[20, 27] Activation of functional APC/C and target specificity are conferred by two WD-40 repeat-containing subunits which act in different phases of the cell cycle. APC/C with substrate-specificity factor Cdc20 is active during G2 and early mitosis, while APC/C with substrate-specificity factor Cdh1 acts during late mitosis and G1 phase. APC/C^{Cdh1} keeps cells in the G1 phase by promoting accumulation of the CKIs $p21^{Cip1}$ and $p27^{Kip1}$, for instance by mediating the degradation of Skp2 and its cofactor Cks1.[27-31] Skp2 and Cks1 are the substrate-targeting subunits of the SCF complex. When Skp2 is associated with the SCF complex, the destruction of $p21^{Cip1}$and $p27^{Kip1}$ is initiated, thereby promoting entry into the S phase. However, when CRL is in complex with the

Fbw7 substrate-recognition factor, it inhibits cell cycle progression by targeting cyclin E for degradation.[20, 25, 27]

In contrast to the RING E3 ligase family, the HECT-domain E3 ligases form temporary covalent bonds with ubiquitin during the ubiquitination process while determining substrate specificity at the same time.[25, 26] As such, HECT domain E3 ligase genes encode for regions that determine both substrate specificity and ligase activity. The E3 ligase UBR5, also known as EDD, EDD1, HYDD, KIAA0896 or DD5, is emerging as a key regulator of the UPS in development and cancer. Both expression of the protein and mutations in the corresponding gene of E3 ligase UBR5, called *UBR5*, are seen in several human cancers.[32-34] *UBR5* has been suggested to act both as a tumor suppressor and as an oncogene, depending on differences in tumor types.[2, 32, 34] Sequencing of tumors has revealed that point mutations in *UBR5* frequently occur throughout the *UBR5* open reading frame and that frameshift mutations tend to occur toward the HECT region of the ligase. The latter would likely result in loss of E3 ubiquitin ligase activity, which suggest that UBR5-mediated ubiquitination has a tumor suppressive role.[2, 32, 34] Whether it promotes or prevents tumor formation may depend on cell-type specific targets. Identification of these targets is particularly challenging and few targets are known at the moment. So far, known targets include the Sox2 transcription factor, $p21^{Cip1}$ and tumor protein 53 (p53).[2, 32-34] Together, protein degradation plays an important role in cell cycle regulation.

In addition to the regulation of protein degradation, chromatin remodeling plays an important role in cell cycle regulation. Chromatin remodeling complexes open or close the nucleosomes in the cell to grant access to transcription factors.[19, 35-37] The complexes are subclasses of Trithorax (TrxG) proteins and are thought to antagonize Polycomb (PcG) group proteins. PcG proteins promote the undifferentiated state of cells, antagonize cell cycle arrest and are considered to be transcriptional repressors. Since TrxG proteins appear to antagonize PcG group proteins, they are considered to be transcriptional activators. The chromatin remodeling complex known as switch/sucrose non-fermenting (SWI/SNF) is part of the TrxG group of proteins and uses the energy generated by ATP hydrolysis to alter nucleosome occupancy at gene regulatory regions.[3, 19, 20, 37] The mammalian SWI/SNF complex exists in three variants: BRGI/BRM-associated factor complexes (BAFs), polybromo-associated BAF complexes (PBAFs), and non-canonical BAFs (ncBAFs). All these complexes contain an ATPase subunit and other subunits that appear to confer tissue specificity.[37, 38] Over the past several years, SWI/SNF has emerged as a major topic of investigation due to the high frequency of mutations in the genes that encode for the complex' subunits. In human tumors, the SWI/SNF complex is the most frequently mutated chromatin remodeling complex.[20, 38-40] The complex is associated with both tumor suppressive and oncogenic roles in cancer development.[3, 19, 20, 37] Moreover, it plays a role in other human diseases, such as neurologic disorders and intellectual disabilities.[38, 39, 41] The extensive role of SWI/SNF in human diseases shows the importance of further understanding how the complex acts on the division of cells and on the regulation of the cell cycle during development.

Several other pathways are frequently found mutated in human cancers and might therefore play a role in the control of cell divisions.[8, 9] One such pathway is the transforming growth factor β (TGF-β) signaling pathway. SMAD4 serves as the central mediator of TGF-β signaling and inhibits epithelial cell proliferation. Mutations in the corresponding gene *SMAD4* have been shown to result in diseases such as cancer. Therefore *SMAD4* is considered to act as a tumor suppressor.[42-46] SMAD4 expression co-regulates the expression of $p21^{Cip1}$ by binding to the promotor of $p21^{Cip1}$ and thereby induces cell cycle arrest.[42-46] Furthermore, it appears that SMAD4 can enhance $p27^{Kip1}$ expression.[47] However, the precise mechanism of the role of *SMAD4* in cell cycle exit remains largely unknown.

The TGF-β pathway shows overlapping targets with p53, which also has been shown to induce transcription of several target genes that are

implicated in cell cycle arrest, such as the gene encoding p21^{Cip1}.[8, 9, 48-51] The various effects of p53 are very complex and its function varies depending on the cell type and on the severity and persistence of genomic damage and cell stress.[8, 9, 50] p53 is known to be post-translationally modified, stabilized and activated in response to cellular stress. When the degree of damage to the genome is excessive, p53 can prevent proliferation of cells or even trigger apoptosis when the damage is irreparable.[8, 9, 48-50] The gene encoding for p53, *p53*, has been extensively studied because of its major role as a tumor suppressor. Mutations in this gene result in functional inactivation of the protein which is seen in more than 50% of human cancers.[8, 9, 50] Consequently, the removal of a key component of the DNA damage sensor takes place, causing disruption of the apoptotic pathway.[8, 9, 50] *p53* has multiple targets and is involved in several processes. Therefore, the direct link to cell cycle progression is not obvious, indicating the relevance of further investigating how it contributes to cell cycle exit.

Many of the insights on the regulation of cell cycle exit have been studied in various model organisms.[52-54] However, not every model organism allows the study of all the aspects of the regulation of cell cycle exit throughout development. For instance, the high cell numbers in developing tissues of the fruit fly *Drosophila melanogaster* make live analysis of cell divisions complicated.[52, 53] In contrast, the relatively simple nematode *Caenorhabditis elegans* is an attractive model system to study the regulation of cell divisions.[3, 55, 56] Despite containing several conserved tissues, *C. elegans* only has 959 somatic cells. Due to this simplicity in cell organization, the entire somatic cell lineage of the animal is known, including the timing of divisions during development, and the position and fate of every daughter cell. Each individual worm goes through four larval stages before reaching adulthood within approximately 3.5 days and the adult can produce 300 identical progeny which all undergo a highly reproducible pattern of cell divisions.[2, 3, 55-57] Combined with the full transparency of the worm, all of these characteristics make *C. elegans* an excellent model system to study how cell division and cell cycle regulation are correlated with developmental stage.

The regulation of cell cycle exit has been studied in several tissues of *C. elegans.*[2, 3, 19, 57] However, the most common type of human cancers is carcinomas, which arise from epithelial tissues.[58] It is therefore important to understand how cell cycle exit is regulated in epithelial cells. *C. elegans* contains several epithelial tissues, including the intestine, the skin and the vulva. However, not all epithelia are suitable for studying the regulation of cell cycle exit. For instance, the intestinal cells enter a cell cycle where mitosis is bypassed during each larval stage. This process is called endoreplication and results in the intrinsic property to re-enter the cell cycle, thereby complicating the study of cell cycle exit regulation alone.[3, 59] The stem cell-like seam cells in the skin are also less attractive to use in cell cycle regulation studies as they maintain the opportunity to proliferate.[3, 56] The cells of the vulval epithelium of *C. elegans,* however, do not undergo endoreplication, nor possess stem cell-like properties. Therefore, this epithelium can be considered as a candidate for studying regulation of cell cycle entry and exit during development.

The vulval epithelium of *C. elegans* is derived from six precursor cells formed in the P lineage, P3.p-P8.p (figure 2). These ventral cord precursor cells (VPCs) are formed during the L1 stage of the worm and remain quiescent until the L3 stage, in which the induction of vulva formation takes place. Starting in the late L2 to early L3 stage, a cell in the somatic gonad, called the anchor cell, secretes the epidermal growth factor (EGF)-related LIN-3. P6.p is closest to the anchor cell and therefore receives the strongest signal of LIN-3. This leads to the activation of multiple cascades and thereby to the adaptation of a primary fate.[2, 3, 56, 60] P5.p and P7.p cells receive lower LIN-3 signals, which eventually results in adapting a secondary fate. The remaining VPCs receive little inductive signaling which induces adaptation of a tertiary fate. The tertiary fate includes a single cell division during L3 stage followed by fusion with the hypodermis.[2, 3, 56, 60]

P5.p-P7.p will undergo several rounds of division in the L3 stage to give rise to a total of 22 vulval cells, which differentiate into seven distinct cell types with specific cell biology and gene expression patterns. The vulva becomes accessible to sperm entry and egg laying at the L4 to adult molt, after invasion of the anchor cell, invagination and connection to the uterus.[2, 3, 56, 60] Together, in a time frame of only hours, all cell divisions are completed and differentiation commences. The vulval epithelium differentiates fast and is not required for viability, hence allowing the study of the contribution of cell cycle regulators to cell cycle exit in *C. elegans*.[2, 3, 56, 60]

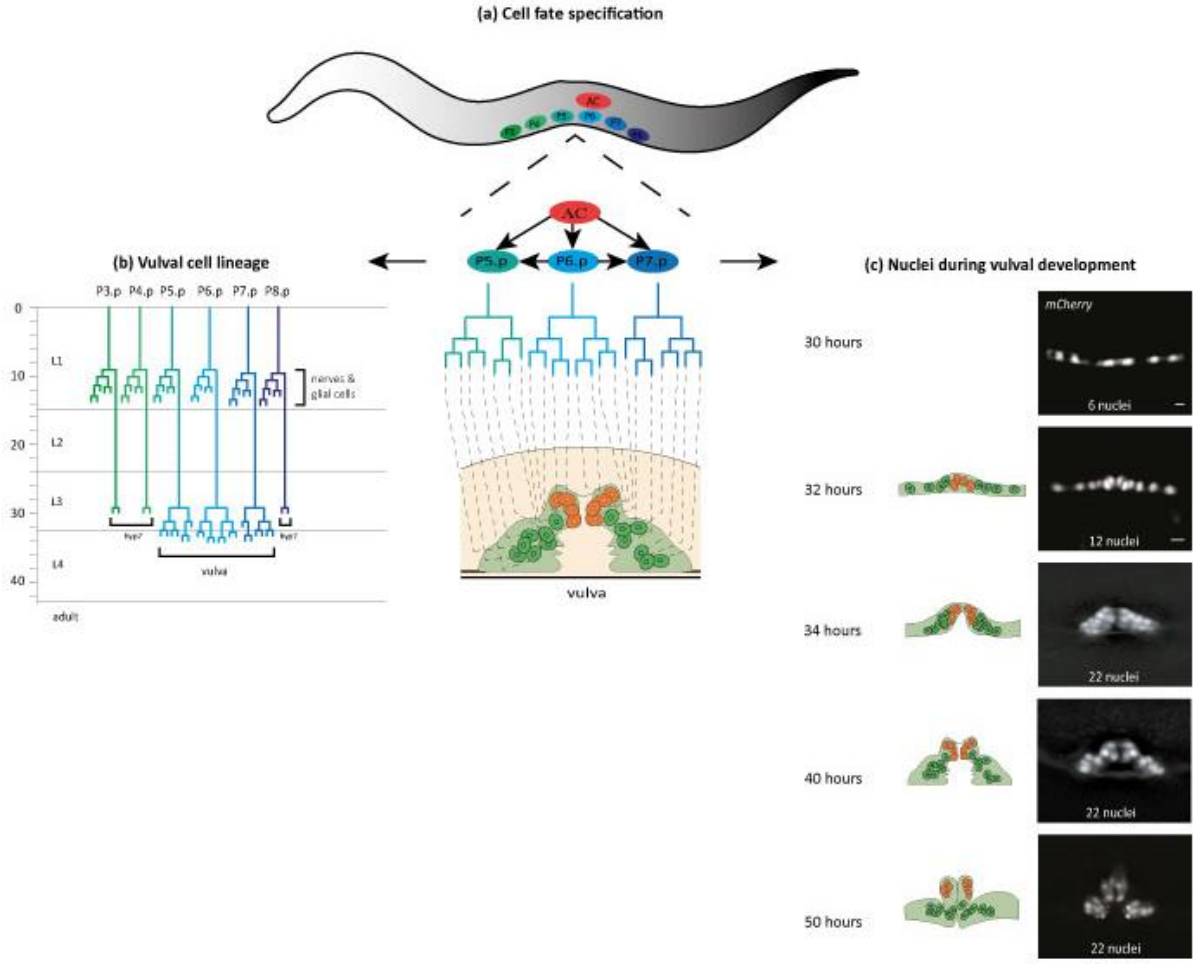

Figure 2. Overview of vulval development. Illustrations adapted from Portegijs et al.[2] **(a)** The vulval epithelium of *C. elegans* is derived from six precursor cells: P3.p-P8.p. The P5.p-P7.p ventral cord precursor cell (VPC) divisions give rise to 22 cells that form the vulva. The anchor cell (AC) secretes the epidermal growth factor (EGF)-related LIN-3. P6.p receives the strongest signal of LIN-3, thereby adapting a primary fate (orange). P5.p and P7.p granddaughters adapt a secondary fate (green) as they receive lower LIN-3 signals. The positions of the nuclei are shown at 40 hours of larval development. The vulval structure is indicated in light green, the dashed lines indicate the position of the cells in the lineage. **(b)** Vulval cell lineages. The y-axis indicates the time (hours) of larval development after hatching. The vertical lines show the P cells and descendants, whereas the horizontal lines show the cell divisions. Hyp7 indicates the hypodermal fusion fate. **(c)** Quantification of vulval divisions. Images at 34-50 hours are maximum projections of Z-stacks.

Many of the cell cycle regulators found in mammals are conserved in *C. elegans* and have been shown to contribute to cell cycle exit in the vulval cell lineage. For instance, several studies described the contribution of two members of the CIP/KIP family in *C. elegans*, called *cki-1* and *cki-2*.[1, 18, 61, 62] These members encode proteins that are equally similar to each other as to human $p21^{Cip1}$ and $p27^{Kip1}$.[1, 18, 61, 62]

In a previous study, vulva specific gene knockout of the cell cycle inhibitor *cki-1* was used to study cell cycle regulation in the vulval epithelium.[2] In a subset of animals, *cki-1* knockout resulted in extra vulval cells. One possible explanation for this phenotype was the compensatory contribution of the related gene *cki-2*. Indeed, levels of the *cki-2* transcript appeared significantly upregulated and

subsequent inactivation of *cki-2* showed a notable increase in the overproliferation of vulval cells. Together, this suggests a strong redundancy between *cki-1* and *cki-2* in controlling cell cycle exit in the vulval cells.[2]

Surprisingly, the aforementioned study also identified a contribution of the homologues of *p53* and *SMAD4*, respectively *cep-1* and *daf-3*, in cell cycle exit in vulval cells of *cki-1* knockouts.[2] In *cki-1* knockouts, inactivation of *cep-1* and *daf-3* alone, but also combined inactivation of *cep-1* and *daf-3* led to a significant overproliferation of vulval cells. This observation was surprising because previous studies have not described a role for these genes in control of the cell cycle in somatic tissues, but only in the germline.[63, 64] Genetic analysis supports a model in which *cep-1* and *daf-3* act upstream of *cki-2*, possibly as part of a compensatory mechanism in response to loss of *cki-1*.[2] The data suggests that *cep-1* and *daf-3* might be involved in the induction of CKIs to promote cell cycle exit, which is similar to the human situation. This project aims to identify how the upregulation of *cki-2* is regulated and whether *cep-1* and *daf-3* play a role in this upregulation.

In the same study an unbiased EMS mutagenesis screen followed by next generation sequencing identified animals with overproliferation of vulval cells that bear a mutation in the gene *ubr-5*.[2] The *ubr-5* gene encodes a homolog of the HECT-domain ubiquitin ligase UBR-5. When combined with a *cki-1* tissue-specific knockout, inactivation of *ubr-5* considerably enhanced the frequency of overproliferation. This indicates that *ubr-5* acts as a cell cycle regulator in *C. elegans,* possibly in parallel to *cki-1*.[2, 32] This project aims to investigate the contribution of *ubr-5* to cell cycle exit and to determine whether it possibly acts as a general regulator of the cell cycle.

In *C. elegans* the BAF and pBAF variants of the chromatin remodeling complex SWI/SNF are conserved and play an important role in the arrest of cell division.[19, 35-37] Knockdown of several key subunits like *swsn-1*, *swsn-4* and *swsn-8*, respectively SMARCC1/2, ATPase subunit and ARID1 in humans, can lead to overproliferation in multiple tissues.[19, 20, 37] When the functionality of the SWI/SNF complex in the mesoblast of *C. elegans* is reduced, cells cannot cease their division in time and fail to differentiate. However, full inactivation of the complex leads to complete cell cycle arrest. Many additional experiments have led to a model that suggests a dosage dependent effect of SWI/SNF on cell cycle regulation, where intermediate levels of SWI/SNF facilitate overproliferation and prevent differentiation, whereas a low or absent dosage of SWI/SNF leads to cell cycle arrest.[3, 19, 37] Making use of mutants that partially inactivate SWI/SNF and thus lead to overproliferation of cells, novel factors can possibly be found that can either rescue the cell cycle disturbances or enhance the degree of proliferation. This project aims to identify factors that work together with the SWI/SNF complex by performing one of several forward genetic screens using mutagenesis of *C. elegans*.

Together, this study will contribute to further understanding the regulation of the cell cycle during the development of *C. elegans*. The identification of mutants and characterization of the mutated genes will lead to more understanding of the targets of the SWI/SNF complex as well as parallel pathways that cooperate or antagonize the function of the SWI/SNF complex. In addition, studying the transcript levels of the CIP/KIP inhibitors upon depletion of *cep-1* and *daf-3* may elucidate whether these genes regulate the expression of CIP/KIP inhibitors and possibly underlie the observed compensatory mechanism between *cki-1* and *cki-2*. Furthermore, this study aims to identify targets of *ubr-5* dependent protein degradation that might contribute to its role in cell cycle exit.

Materials and methods

C. elegans strains and culture conditions

C. elegans strains were kept on 6 cm petri dishes with nematode growth medium (NGM) agar and fed with *Escherichia coli* OP50.[55] The genotypes of the used strains can be found in Supplementary Table 1 (S1). Unless stated otherwise, all the animals were maintained at 20°C.

Genetic crosses

cep-1 ; daf-3 double mutant strains were generated by genetically crossing[55] and checked by polymerase chain reaction (PCR) (for used primers see table S2). The used strains for these crosses were SV2243 *cep-1 (gk138)* I ; *cki-1*^{LOX} II ; *he317* [read-out Blue to red] IV ; *heSi220* [*plin-31*::CRE] X and SV2467 *he317* [read-out Blue to Red] IV ; *daf-3 (ok3610) heSi220* [*plin-31*::CRE] X.

The SV2478 *swsn-8*^{Lox} *; he317* [read-out Blue to Red] IV *; heSi220* [*plin-31*::CRE] X strain was generated by genetically crossing strain SV21930 *swsn-8*^{Lox} *heSi141* [*Phlh8*::CRE]X and strain SV2071 *he317* [read-out Blue to Red] IV *; heSi220* [*plin-31*::CRE] X (for full genotype see table S1). Progeny of successful crosses were checked by PCR (for used primers see table S2) and fluorescence microscopy. Homozygous animals were selected.

The SV2481 *ubr-5 (he332)* I ; *cki-1* (*he329* [*cki-1*^{loxP}]) II ; *he317* [read-out Blue to red] IV ; *heSi220* [*plin-31*::CRE] X strain was generated by genetically crossing SV2480 *ubr-5 (he332)* I ; *he317* [read-out Blue to red] IV ; *heSi220* [*plin-31*::CRE] X and SV2080 *cki-1* (*he329* [*cki-1*^{loxP}]) II ; *he317* [*peft-3*-lox^{2272}NLS::BFP::*let-858* UTR^{lox2272}-NLS::mCherry] IV ; *heSi220* [*plin-31*::CRE] X and checked by both PCR and sequencing (for used primers see table S2).

lin-31::CRE recombination reporter

A reporter that expresses blue fluorescent protein (BFP) in the nucleus of all cells, yet switches upon CRE-mediated recombination to mCherry expression, was used to aid analysis of the vulval lineages. A single-copy transgene expressing CRE under the control of the *lin-31* promotor was integrated to induce mCherry specifically in the vulval lineages (figure S1). The specificity of switching in the vulval lineage was researched by Portegijs et al. (2019) and showed suitable for easy tracing and quantification of cell divisions in the vulval epithelium.[2, 37] Hence forth strain SV2071 *he317* [*peft-3*-lox^{2272}NLS::BFP::*let-858* UTR^{lox2272}-NLS::mCherry] IV ; *heSi220* [*plin-31*::CRE] X is referred to as wild type.

CRISPR/Cas9 mediated genome editing

CRISPR/Cas9 RNA genome editing was performed in SV2071 *he317*[*peft-3*-lox^{2272}NLS::BFP::*let-858* UTR^{lox2272}-NLS::mCherry] IV ; *heSi220* [*plin-31*::CRE] X to recreate the *ubr-5* point mutation that was identified in the EMS screen[2]. This guanine to adenine (G>A) point mutation was introduced in the first base of intron 25, located in the HECT domain of *ubr-5*. The gonads of young adults were injected with a solution containing the following injection mix[65]: 0.5µl Cas9 of 10µg/µl stock, 5µl tracrRNA of 0.4µg/µl stock, 2.8µl crRNA of 0.4µg/µl stock (1.4µl of both OVP736 and OVP737, see table S2), 2.2µl of a single stranded DNA repair template with 35 base pairs overhang around the site of editing (1µg/µl stock), 1.6µl PRF4::*rol-6* (*su1006*) plasmid of 500ng/µl stock and 7.9µl nuclease free water. On a plate with injected animals, the number of F1 rollers was assumed as a reliable metric for the quality of the injections. The plates with the highest number of rollers were chosen after about three days at 20°C. 24 worms per plate, both rollers and non-rollers, were picked to new plates. These F1 worms were allowed to lay eggs at 20°C for two days and were then used to perform worm lysis. Next, PCR was performed with primers (OVP717 and OVP735, see S2) diagnostic for a successfully edited genome. The correct incorporation of the mutation was confirmed by sequencing (*Macrogen*) using 7.5µl purified PCR product (primers OVP716 and OVP717, see S2) and 2.5µl diluted OVP716 (0.4µg/µl stock).

Similarly, CRISPR/Cas9 RNA genome editing was performed in SV2071 *he317* [*peft-3*-lox^{2272}NLS::BFP::*let-858* UTR^{lox2272}-NLS::mCherry] IV ; *heSi220* [*plin-31*::CRE] X to introduce new *cki-1*^{Lox} sites. The following solution[65] was injected in the gonads of young adults: 0.5µl Cas9 of 10µg/µl stock, 5µl tracrRNA of 0.4µg/µl stock, 2.8µl crRNA of 0.4µg/µl stock (1.4µl of both OVP738 and OVP739, see table S2), 5µl dsDNA (100ng/µl stock), 1.6µl PRF4::*rol-6* (*su1006*) plasmid of 500ng/µl stock and 5.1µl nuclease free water. The used dsDNA was obtained by performing SV2080 *cki-1* (*he329* [*cki-1*^{loxP}]) II ; *he317* [*peft-3*-lox^{2272}NLS::BFP::*let-858* UTR^{lox2272}-NLS::mCherry] IV ; *heSi220* [*plin-31*::CRE] X worm lysis, followed by PCR (primers OVP740

and OVP741, see S2) and isolation of the DNA using the Qiagen MinElute kit. On a plate with injected animals, the number of F1 rollers was assumed as a reliable metric for the quality of the injections. The plates with the highest number of rollers were chosen after about three days at 20°C. 24 worms per plate, both rollers and non-rollers, were picked to new plates. These F1 worms were allowed to lay eggs at 20°C for two days and were then used to perform worm lysis. Next, PCR was performed with primers (OMG154 and OVP742, see S2) diagnostic for a successfully edited genome. The correct incorporation of the mutation was confirmed by sequencing (*Macrogen*) using 7.5µl purified PCR product (primers OMG154 and OVP742, see S2) and 2.5µl diluted OMG154 (0.4µg/µl stock).

Microscopy and quantification of cell numbers
All animals were synchronized using hypochlorite treatment (bleaching). L1 arrest synchronized animals were grown at 20°C for 40 hours before analyzing them using the Zeiss Axioplan fluorescence microscope. For analysis and quantification, worms of the strains were first washed off of plates using M9 medium with 0.05% Tween-20 (hence forth referred to as M9-T) and centrifuged at 1350 rpm for 1 minute. The worms (2.5µl of the pellet) were mounted on 3% agarose slides using 2.5µl tetramisole. Z-stacks were taken using a 63x/1.4NA lens on the Zeiss Axioplan fluorescence microscope, with a slice interval of 0.40µm and a light intensity of 40ms. Extra vulval cell divisions were quantified using ImageJ software, by counting the number of mCherry-positive cells visible in Z-stacks. Images were processed by subtracting a Gaussian-blur filtered image (Sigma (Radius): 20) from the Z-stack.

Ethyl Methane Sulfonate (EMS) mutagenesis
Ethyl Methane Sulfonate (EMS) mutagenesis was performed in strain SV2478 *swsn-8^{Lox} ; he317* [read-out Blue to Red] IV *; heSi220* [*plin-31*::CRE] X. Animals of this strain were collected in 3ml M9-T, followed by the addition of 20 µl ethyl methane sulfonate mixed with 1ml M9-T and incubated at room temperature for 4 hours. Next, the animals were washed and centrifuged (1350 rpm for 1 minute) 3 times using 4ml M9-T during each washing step. Subsequently, the animals were placed on NGM plates with OP50. From these plates L4 animals were picked onto 10 new plates (3 worms per plate). These animals were grown at 20°C for 4 days, before picking 600 F1 worms to new plates (3 animals per plate). These F1 worms were grown at 20°C for 1 week. Then, the progeny was observed. Bagging worms were picked to new plates and grown at 20°C for 1 week. The F3 worms that were bagging, were picked to new plates and grown at 20°C for 4 days before observing the worms using a 63x/1.4NA lens on the Zeiss Axioplan fluorescence microscope. This procedure was performed twice. During the second EMS mutagenesis 400 F1 worms (instead of 600) were picked to new NGM plates (2 animals per plate). In total, 2000 haploid genomes were set up for screening. However, the number of haploid genomes screened is lower due to sterility caused by EMS and due to plates unable to be screened because of technical reasons such as starvation.

Statistical analysis
All available animals of the right stage and genotype were counted, hence the sample sizes were not pre-determined. Cell numbers are included from at least 50 independent animals, except for strain SV2481 *ubr-5 (he332)* I ; *cki-1* (*he329* [*cki-1^{loxP}*]) II ; *he317* [read-out Blue to red] IV ; *heSi220* [*plin-31*::CRE] X, of which 38 independent animals were observed. By using GraphPad Prism 8.4.3 the graphs and data analysis were produced. Plots indicate all data points, as well as the mean (average) ± Standard Deviation (SD). Unpaired two-tailed Student's t tests with Welch's correction were performed to research statistical significance of the difference between means, since the data essentially fit normal distributions. P values: **** P<0.0001, *** P<0.001, ** P<0.01, * P<0.05, ns not significant.

Results

New cki-1^{Lox} animals have fewer vulval cells than the originally generated cki-1^{Lox} animals
In a previous study, a strong redundancy between *cki-1* and *cki-2* in controlling cell cycle exit in the vulval cells was suggested.[2] In a

subset of animals, *cki-1* knockout resulted in extra vulval cells. One possible explanation for this phenotype was the compensatory contribution of the related gene *cki-2*. Indeed, subsequent inactivation of *cki-2* showed a notable increase in the overproliferation of vulval cells. In addition, Single Molecule Fluorescence In Situ Hybridization (smFISH) experiments showed a significant upregulation of *cki-2* RNA transcripts in the absence of *cki-1*.[2] The question remained how the levels of *cki-2* transcript were upregulated. The *cki-1* and *cki-2* genes are separated by only a 4871 base pairs intergenic region and thus are very closely linked (figure 3a). An explanation for the upregulation of *cki-2* could be read-through of Polymerase II activity, which normally terminates in the *cki-1* 3' untranslated region (UTR). It could be that important regulatory sequences that normally prevent *cki-2* transcription were removed in the *cki-1^{Lox}* allele. In this allele the second intron of *cki-1* and a 622 base pairs region downstream of *cki-1* containing the 3'UTR were excised. The excised region in the *cki-1^{Lox}* allele could have affected the downstream located *cki-2*. To study this possibility, a new version of *cki-1*, with a much smaller deletion than before, was engineered by CRISPR/Cas9 mediated genome editing (figure 3b). A significant reduction in the number of vulval nuclei of new *cki-1^{Lox}* animals was observed when compared to the originally generated *cki-1^{lox}* and wild type animals (figure 3d). These findings are contrary to the hypothesis where an overproliferation of vulval cells was expected. One of the explanations for these findings could be that the sequence where the Lox site was placed, is important for a successful transcription. However, it is interesting to note that most new *cki-1^{Lox}* animals (26,5%) had only 14 vulval nuclei (figure 3e), but the shape of a normal 22 nuclei vulva (figure 3c). A wide range of vulval nuclei numbers, ranging from 11 to 26, was seen (figure 3e). However, the vulvae did seem functional as the worms did not show the bagging phenotype. In conclusion, it appears that the new *cki-1^{Lox}* animals have fewer vulval cells than the originally generated *cki-1^{Lox}* animals.

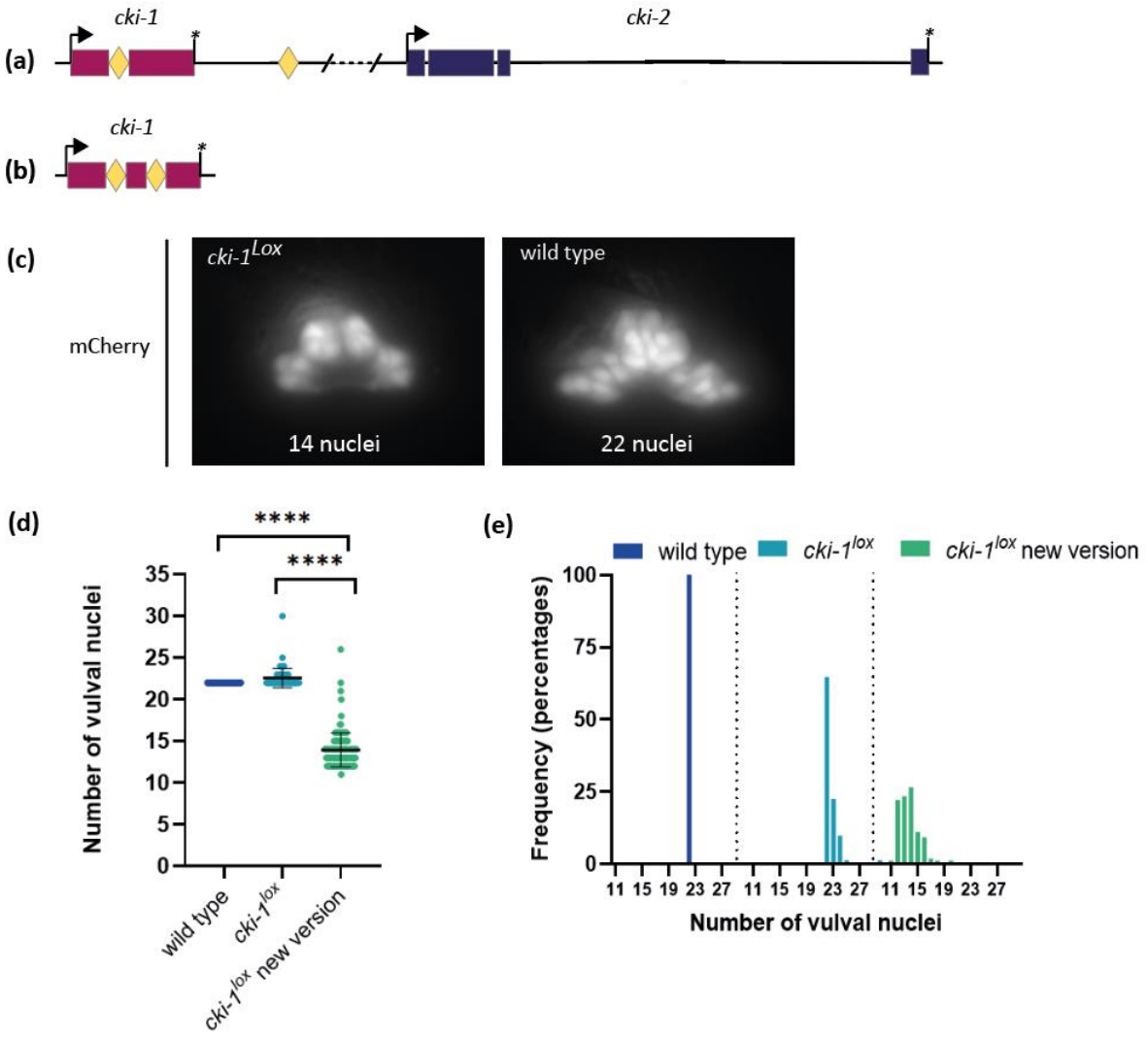

Figure 3. Lineage-specific inactivation of *cki-1*

A) Graphic representation of the *cki-1* and *cki-2* locus on chromosome II. The *cki-1* and *cki-2* genes are separated by only a 4871 base pairs intergenic region. The Lox site integration is indicated by the yellow diamonds. The arrows indicate the start of transcription whereas the asterisks indicate transcriptional stop.

B) Graphic representation of the generated *cki-1*. Two Lox sites are integrated, which is indicated by the yellow diamonds. The arrows indicate the start of transcription whereas the asterisks indicate transcriptional stop.

C) Representative images of reporter expression in *cki-1* new version and wild type animals. 26.5% of the *cki-1* new version animals showed 14 vulval nuclei whereas 22 vulval nuclei is seen in wild type animals. Images are maximum projections of Z-stacks. Anterior-posterior orientation is unknown.

D) Quantification of the number of vulval nuclei in wild type animals, *cki-1*^{Lox} animals and *cki-1*^{Lox} new version animals (respectively SV2071, SV2080 and SV2483, see table S1). The Y-axis represents the number of vulval nuclei. Error bars: mean ± SD. Each dot represents a single animal. Statistical analyses: unpaired Students t tests with Welch's correction. P value **** P<0.0001.

E) Frequency distribution of the number of vulval nuclei in wild type animals, *cki-1*^{Lox} animals and *cki-1*^{Lox} new version animals. The Y-axis represents the frequency in percentages of vulval nuclei numbers. The X-axis represents the number of vulval nuclei.

Loss of both cep-1 and daf-3 in cki-1 knockouts did not shift the frequency of animals with extra vulval cell divisions

The aforementioned study also identified a contribution of the homologues of *p53* and *SMAD4*, respectively *cep-1* and *daf-3* in *C. elegans*, in cell cycle exit in vulval cells of *cki-1* knockouts.[2] In this study, RNA-mediated interference (RNAi) was performed by dsRNA microinjections in the animals. In *cki-1* knockouts, inactivation of *cep-1* and *daf-3* alone, but also combined inactivation of *cep-1* and *daf-3* led to a significant overproliferation of vulval cells. In addition, loss of both *cep-1* and *daf-3* further increased the number of *cki-1* animals with extra vulval cells when compared to loss of *cki-1* alone. To further clarify how *cep-1* and *daf-3* contribute in cell cycle exit in vulval cells, knockout mutants were engineered and vulval cells were quantified. Loss of *cep-1*, *daf-3* and combined loss of *cep-1* and *daf-3* did not lead to a

significant overproliferation in the vulval epithelium compared to the wild type (figure 4a, blue). In a *cki-1* knockout situation, loss of *cep-1*, *daf-3* and combined loss of *cep-1* and *daf-3* did lead to a significant increase of vulval cells compared to the wild type (figure 4a). This shows that the activity of *cki-1* is important for preventing overproliferation in the vulval lineage, as was also seen in the aforementioned study.[2] However, in contrast to the previous study, simultaneous loss of *cep-1*, *daf-3* and *cki-1* did not lead to a significant overproliferation of vulval cells compared to loss of only *cki-1* (figure 4a, green). In fact, 68.6% of the animals in this condition, had the normal amount of vulval nuclei (22 nuclei) (figure 4b). In conclusion, loss of both *cep-1* and *daf-3* in *cki-1* knockouts did not shift the frequency of animals with extra vulval cell divisions compared to loss of *cki-1* alone.

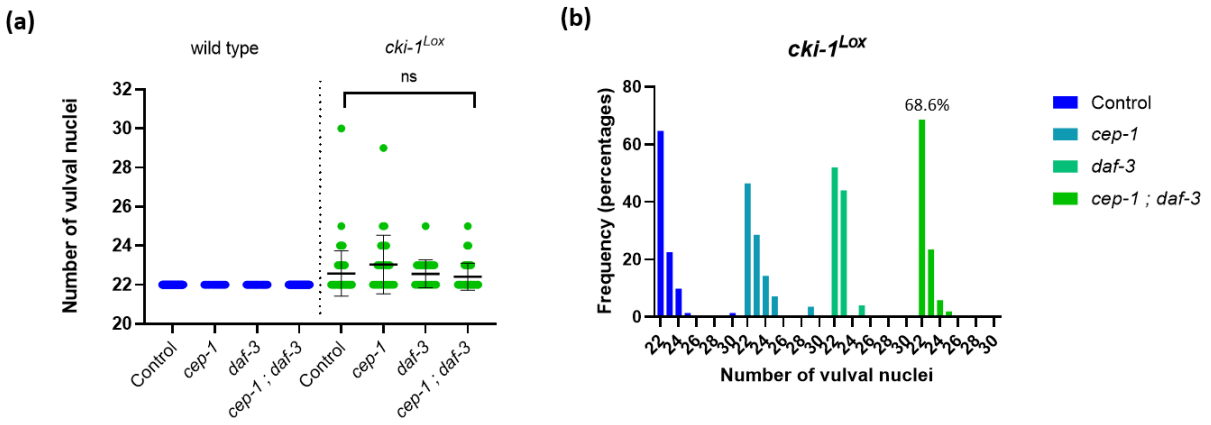

Figure 4. Lineage-specific inactivation of *cep-1, daf-3* and *cki-1*

A) Quantification of the number of vulval nuclei in wild type, *cep-1, daf-3* and *cep-1 ; daf-3* animals (blue, respectively SV2071, SV2242, SV2467 and SV2476) and *cep-1, daf-3* and *cep-1 ; daf-3* animals combined with inactivation of *cki-1*^{Lox} (respectively SV2080, SV2243, SV2468 and SV2477, see table S1). The Y-axis represents the number of vulval nuclei. Error bars: mean ± SD. Each dot represents a single animal. Statistical analyses: unpaired Students t tests with Welch's correction. P values: **** P<0.0001, *** P<0.001, ** P<0.01, * P<0.05, ns not significant.

B) Frequency distribution of the number of vulval nuclei in *cki-1*^{Lox}, *cep-1, daf-3* and *cep-1 ; daf-3 ; cki-1*^{Lox} animals. The Y-axis represents the frequency in percentages of vulval nuclei numbers. The X-axis represents the number of vulval nuclei.

ubr-5 contributes to cell cycle arrest

In the study by Portegijs et al. (2019) animals with overproliferation of vulval cells that bear a mutation in the gene *ubr-5* were identified by performing an unbiased EMS mutagenesis screen followed by next generation sequencing. The function of this gene was disrupted by dsRNA injections in order to test whether *ubr-5* contributes to cell cycle control. In a subset of animals, RNAi of *ubr-5* caused extra division of vulval cells. Combined inactivation of both *cki-1*^{Lox} and *ubr-5* considerably enhanced the frequency of overproliferation in the vulval epithelium, which suggested a redundancy between *cki-1* and *ubr-5*.[2] By CRISPR/Cas9 mediated genome editing, a strain was generated with a point mutation in the HECT domain of *ubr-5*. Loss of *ubr-5* did not lead to a significant overproliferation in the vulval epithelium compared to the wild type (figure 5a). However, it did lead to a small population of animals in which the cell cycle was not fully arrested, leading to several extra vulval nuclei (figure 5). Even though the results were not statistically significant, the results can be of clinical significance. Loss of *ubr-5* occasionally resulted in progeny with more than 22 vulval nuclei, which suggests that *ubr-5* has a function as an inhibitor of cell cycle exit. In addition, combined inactivation of *cki-1*^{Lox} and *ubr-5* led to a significant increase of vulval cells compared to the wild type (P<0.05).

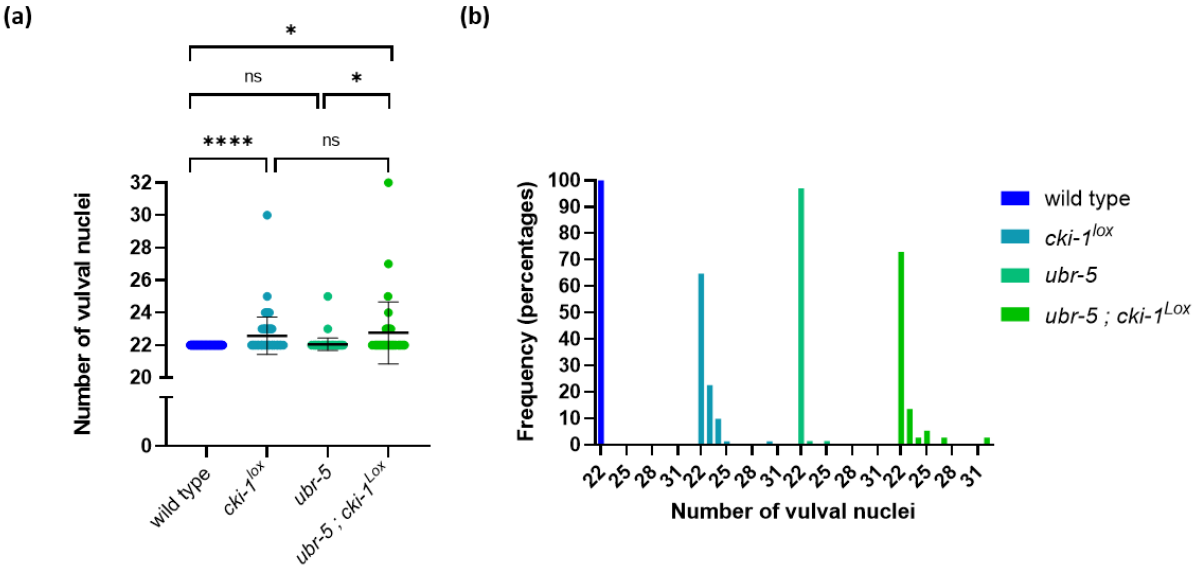

Figure 5. Lineage-specific inactivation of *ubr-5*

(A) Quantification of the number of vulval nuclei in wild type, *cki-1*^{Lox}, *ubr-5* and *ubr-5 ; cki-1*^{Lox} animals (respectively SV2071, SV2080, SV2480 and SV2481, see table S1). The Y-axis represents the number of vulval nuclei. Error bars: mean ± SD. Each dot represents a single animal. Statistical analyses: unpaired Students t tests with Welch's correction. P values: **** P<0.0001, *** P<0.001, ** P<0.01, * P<0.05, ns not significant.

(B) Frequency distribution of the number of vulval nuclei in wild type, *cki-1*^{Lox}, *ubr-5* and *ubr-5 ; cki-1*^{Lox} animals. The Y-axis represents the frequency in percentages of vulval nuclei numbers. The X-axis represents the number of vulval nuclei.

Loss of swsn-8 significantly leads to overproliferation of vulval cells

Multiple experiments have led to a model that suggests a dosage dependent effect of SWI/SNF on cell cycle regulation, where intermediate levels of SWI/SNF facilitate overproliferation and prevent differentiation, whereas a low or absent dosage of SWI/SNF leads to cell cycle arrest.[3, 19, 37] Previous work in *C. elegans* has shown that inactivation of *swsn-1* can lead to overproliferation of the early dividing body wall muscle precursors (mesoblast), whereas it can lead to cell division arrest of the late dividing egg-laying muscle precursor cells (vulva). Loss of *swsn-8* gave the same effect as *swsn-1* although it showed a less strong overproliferation in the mesoblast and a less strong halt of proliferation in the vulva compared *swsn-1*.[37] In this study the role of *swsn-8* in the regulation of proliferation was examined. Loss of *swsn-8* significantly led to overproliferation in the vulval epithelium compared to the wild type (figure 6a). Additional cell divisions were limited in number, but occurred in nearly 40% of the observed animals (figure 6b). This indicates that *swsn-8* is important for cell cycle arrest during development.

EMS mutagenesis screen results in promising aberrant phenotypes of C. elegans' vulva

Upon quantification of *swsn-8* animals, worms with the bagging phenotype were seen occasionally, which could be the result of less proliferation or overproliferation of vulval cells. Based on the bagging phenotype, an EMS mutagenesis screen was performed to find factors that either rescue the cell cycle disturbances or enhance the degree of proliferation. Occasionally progeny of mutagenized worms showed aberrant vulvae (figure 6c), including additional vulval nuclei. However, due to time constraints caused by the outbreak of COVID-19, the aberrant vulvae were not further investigated. Additional research, e.g. whole genome sequencing, is required to identify the genes causing the observed phenotypes.

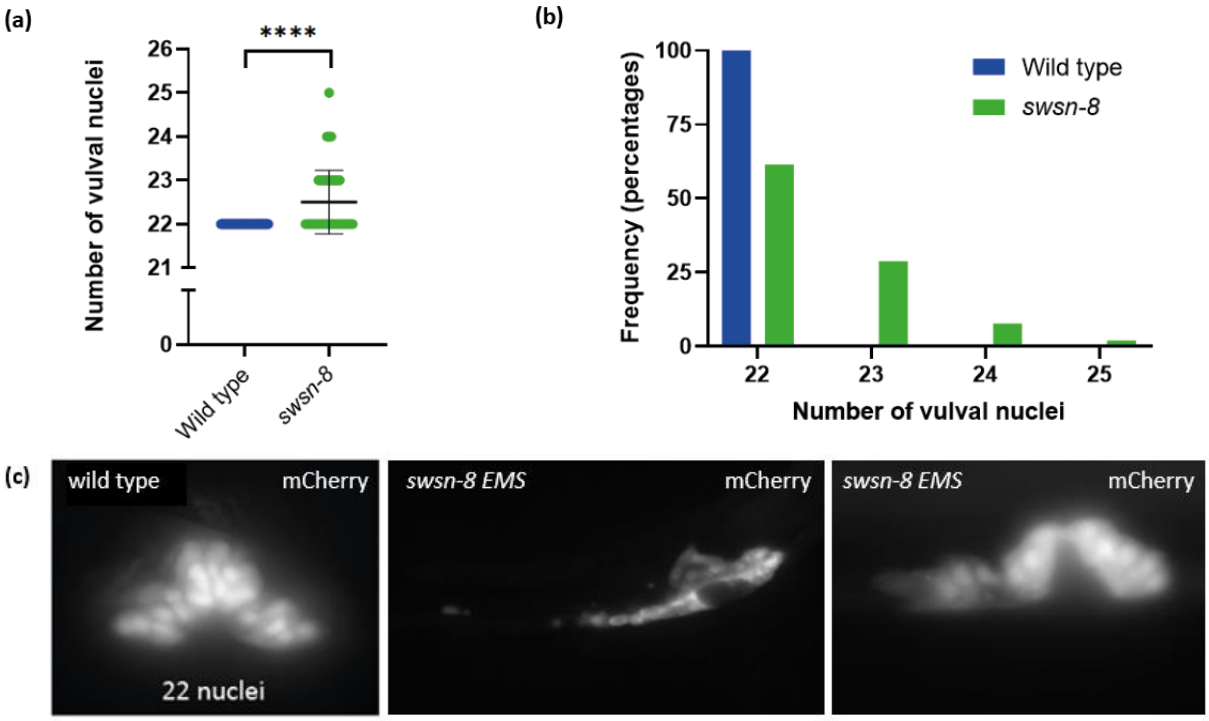

Figure 6. EMS mutagenesis screen using inactivated *swsn-8*

A) Quantification of the number of vulval nuclei in wild type and *swsn-8* animals (respectively SV2071 and SV2478, see table S1). The Y-axis represents the number of vulval nuclei. Error bars: mean ± SD. Each dot represents a single animal. Statistical analyses: unpaired Students t tests with Welch's correction. P values: **** P<0.0001, *** P<0.001, ** P<0.01, * P<0.05, ns not significant.

B) Frequency distribution of the number of vulval nuclei in wild type and *swsn-8* animals. The Y-axis represents the frequency in percentages of vulval nuclei numbers. The X-axis represents the number of vulval nuclei.

C) Representative images of aberrant vulvae found in the EMS screen of *swsn-8* animals. The left image shows the vulva of a wild type animal (maximum projection of Z-stacks). The middle image shows an abnormal vulval shape. The vulva in the right image seems to have extra vulval nuclei. The middle and right Images are fragments of Z-stacks. Anterior-posterior orientation is unknown.

Discussion

Several pathways are frequently found mutated in human cancers and might therefore play a role in the control of cell divisions.[8, 9] In *C. elegans,* many of the cell cycle regulators found in mammals are conserved.[2, 16, 37, 64] This study aimed to identify how the upregulation of *cki-2* is regulated and whether *cep-1* and *daf-3* play a role in this upregulation. Loss of *cep-1, daf-3* and combined loss of *cep-1* and *daf-3* did not lead to a significant overproliferation in the vulval epithelium compared to the wild type (figure 4a). In a *cki-1* knockout situation, loss of *cep-1*, *daf-3* and combined loss of *cep-1* and *daf-3* did lead to a significant increase of vulval cells compared to the wild type. This shows that the activity of *cki-1* is important for preventing overproliferation in the vulval lineage, as was also seen in the aforementioned study.[2] In contrast to the previous study, simultaneous loss of *cep-1*, *daf-3* and *cki-1* did not lead to a significant overproliferation of vulval cells compared to loss of *cki-1* alone (figure 4a). Therefore the question remains what the precise role *cep-1* and *daf-3* is in cell cycle exit. To further study the effect of *cep-1* and *daf-3* on *cki-1* and *cki-2*, smFISH experiments were scheduled to detect the number of *cki-1* and *cki-2* mRNA transcripts in vulval cells. However, due to technical constraints caused by the outbreak of COVID-19 these experiments were not performed. In conclusion, loss of both *cep-1* and *daf-3* in *cki-1* knockouts did not shift the frequency of animals with extra vulval cell divisions compared to loss of *cki-1* alone. However, considering *p53* and *SMAD4* have an effect on $p21^{Cip1}$ and $p27^{Kip1}$, it is attractive to believe *cep-1* and *daf-3* might have an effect on *cki-1* and *cki-2*.[30, 32, 33, 51] These assumptions might be further addressed in future studies. Future studies could include generating a *cki-2* knockout with inactivation of *cep-1, daf-3* and *cki-1*, and a combined inactivation of these genes. In addition, smFISH experiments might provide insights in the mechanism of action of *cep-1* and *daf-3*.

Another explanation for the upregulation of *cki-2* transcript levels that was found in the aforementioned study[2] could be read-through of Polymerase II activity, which normally terminates in the *cki-1* 3' untranslated region (UTR). It could be that important regulatory sequences that normally prevent *cki-2* transcription were removed in the *cki-1*^{Lox} allele. As this would affect the experiments excessively, this project studied that possibility. A new version of *cki-1* was engineered by CRISPR/Cas9 mediated genome editing (figure 3), involving a much smaller deletion than before. Surprisingly, a significant reduction of vulval cells was found when compared to the wild type (figure 3). One of the explanations for these findings could be that the sequence where the new Lox site is placed, is important for a successful transcription. However, that probably does not explain why the vulvae had normal shapes. Even though the majority had less than 22 vulval nuclei, all the vulvae had normal shapes. In addition, a wide range of vulval nuclei numbers was observed (ranging from 11 to 26 vulval nuclei). However, the vulvae did seem functional as the worms did not show the bagging phenotype. Future research should further develop the new *cki-1* version, including engineering a *cki-1* new version ; *cki-2* strain. The latter shall help distinguish between the possibility of an altered *cki-2* transcription and for instance the induction of *cki-2* by *cep-1* and *daf-3*.

Furthermore, this study aimed to identify targets of *ubr-5* dependent protein degradation that might contribute to its role in cell cycle exit. The aforementioned study suggested a redundancy between *cki-1* and *ubr-5*, partly based on the fact that combined inactivation of both *cki-1*^{Lox} and *ubr-5* led to a significant increase of vulval cells compared to the wild type.[2] In this study, the combined inactivation of *cki-1*^{Lox} and *ubr-5* led to a significant increase of vulval cells as well. Contrary to the prior study, loss of *ubr-5* alone did not lead to a significant overproliferation in the vulval epithelium compared to the wild type (figure 5). Comparing this study with the prior study, the difference in significance could be explained by the methods used to silence the genes. In the aforementioned study, RNAi was performed to silence *ubr-5* whereas in this study CRISPR/Cas9 mediated genome editing was performed to permanently disrupt the gene. Even though loss of *ubr-5* alone did not lead to a statistically significant overproliferation of vulval cells, it did occasionally result in progeny with more than 22 vulval nuclei (figure 5). The results are therefore of clinical significance as it suggests that *ubr-5* contributes to cell cycle arrest. In humans UBR5 has been suggested to act both as a tumor suppressor and as an oncogene, depending on differences in tumor types. Point mutations in *UBR5* frequently occur throughout the *UBR5* open reading frame and frameshift mutations tend to occur toward the HECT region of the ligase. Whether it promotes or prevents tumor formation may depend on cell-type specific targets. [2, 32, 34] If this applies for *ubr-5* in *C. elegans* as well has yet to be determined. Further studies need to be carried out in order to determine the precise role and targets of *ubr-5* in *C. elegans*.

Moreover, this study aimed to identify factors that work together with the SWI/SNF complex by performing forward genetic screens using mutagenesis of *C. elegans.* Previous work in *C. elegans* has shown that inactivation of *swsn-1* can lead to both extra cells and fewer cells in the mesoblast and vulva.[37] However, in the vulva it is much more common that cells prematurely exit the cell cycle resulting in fewer vulval cells. Loss of SWI/SNF subunit *swsn-8* showed a similar trend, though a less pronounced overproliferation and cell cycle arrest compared to the effect of loss of *swsn-1*.[37] In this study, specifically the role of SWI/SNF subunit *swsn-8* in the regulation of proliferation was examined. *swsn-8* is a subunit of the BAF variant of SWI/SNF and is predicted to contribute to nucleosome binding activity. In addition, it is involved in the positive regulation of transcription by RNA polymerase II and in nematode larval development.[37, 70] Loss of *swsn-8* significantly led to overproliferation in the vulval epithelium compared to the wild type (figure 6), indicating that *swsn-8* is important for cell cycle arrest during development. This overproliferation phenotype could be used to find factors that either rescue the cell cycle disturbances or

enhance the degree of proliferation. However, due to time constraints caused by the outbreak of COVID-19, performing a screen for overproliferation was not an option. Instead an EMS screen was performed based on the bagging phenotype as upon quantification of *swsn-8* animals, worms with the bagging phenotype were seen occasionally. The bagging phenotype could be caused by parallel inactivation of the SWI/SNF complex. In total, 2000 haploid genomes were set up for screening. However, the actual number of haploid genomes screened was lower due to sterility caused by EMS and due to plates unable to be screened because of technical reasons such as starvation. Starved animals exhibit morphological characteristics, like a faint appearance, that are the outcome of nutrient deprivation. These animals arrest their development and disperse in order to search for food.[56, 71] Therefore, starved worms are unreliable and thus were excluded from this experiment. Nonetheless, multiple aberrant vulvae were observed (figure 6c), including additional vulval nuclei. Further research, for instance whole genome sequencing, should be carried out to identify the genes that caused the observed phenotype.

The approach utilized for quantifying vulval nuclei suffers from the limitation that it is done manually and is therefore subject to human error. This means that the outcome can be rather subjective when, for instance, some vulval nuclei hardly appear, but are definitely present. Therefore, it is recommended to verify all made images by a second party to increase the accuracy of the quantified vulval nuclei. Additionally, all vulval nuclei were quantified at a relatively early time point (40 hours). It is reasonable to believe that the number of vulval cells increases over time when cell cycle arrest remains impaired. Therefore it would be promising to observe the vulval epithelium at a later time point. However, quantifying the cells at later stages is less reliable due to morphological changes and toroid fusion. Preventing these changes could allow quantification of vulval nuclei at later timepoints and help determine the long-term effects of depletion of cell cycle inhibitors. The EGFR/RAS/MAPK signaling pathway and LIN-39 are important for specifying cell fates during vulval induction and regulate various aspects of epidermal morphogenesis. Both continue to act during the subsequent phase of cell fate execution and can thus help in preventing vulval changes.[2, 72] Further investigation and experimentation at a later time point is strongly recommended.

Another study that would be worthwhile, is following up the locations of overproliferation of vulval cells within the vulva. In a prior study[2], a follow up on the overproliferation locations of *cep-1* and *daf-3* (RNAi) showed that P5.ppp and P7.paa most commonly fail to arrest the cell cycle in loss of CKI mutants. In this study however, the locations of overproliferation of vulval cells were not researched due to time constraints. Knowing precisely where in the vulva the overproliferation takes places, might provide insights in the mechanisms of cell cycle exit in a developing tissue and thus is strongly recommended to further research.

In summary, this study has contributed to further understanding the regulation of the cell cycle during the development of the vulva of *C. elegans.* The results provide evidence for a contribution of *ubr-5* in cell cycle arrest. However, the mechanism by which this occurs must be further researched, as well as the effects of *cep-1* and *daf-3* on cell cycle exit. The question remains how the upregulation of *cki-2* is regulated and whether *cep-1* and *daf-3* play a role in this upregulation. Additionally, loss of *swsn-8* significantly led to overproliferation of vulval cells compared to the wild type. It seems to be a promising gene to further investigate in order to identify targets of the SWI/SNF complex as well as parallel pathways that cooperate or antagonize the complex' function. To conclude, using the model organism *C. elegans*, new insights in how cell cycle exit is controlled were found that can be central to our understanding of why defects in genes responsible for cell cycle exit could cause cells to continue to divide.

Acknowledgements

I would like to thank all members of the Van den Heuvel and Boxem groups of the Developmental Biology division of Utrecht University for input, discussion and comments on the performed experiments. Especially, I would like to thank Dr. V.C. Portegijs for teaching me everything about the wormies, for guiding a beginner like me, for giving me the necessary feedback and for encouraging me.

Supplementary

Table S1. Overview of used *C. elegans* strains

Strain	Genotype
N2	Wild type
SV1930	*swsn-8* (*he273* [loxN exon3])I; *swsn-8* (*he287* [loxN last intron])I; *heSi208* [*Peft-3*::LoxP::NLS *egl-13*::tagBFP2::*tbb-2* UTR::LoxP::NLS *egl-13*::mCherry:: *tbb-2* UTR]V; *heSi141* [*Phlh8*::CRE]X
SV2071	*he317* [*peft-3*-lox2272NLS::BFP::*let-858* UTRlox2272-NLS::mCherry] IV ; *heSi220* [*plin-31*::CRE] X
SV2080	*cki-1* (*he329* [*cki-1loxP*]) II ; *he317* [*peft-3*-lox2272NLS::BFP::*let-858* UTRlox2272-NLS::mCherry] IV ; *heSi220* [*plin-31*::CRE] X
SV2179	*cki-1LoxP ; cki-2 (he352[cki-2LoxP])* II *; he317* [read-out Blue to red] IV *; heSi220* [*plin-31*::CRE] X
SV2242	*cep-1 (gk138)* I ; *he317* [read-out Blue to red] IV ; *heSi220* [*plin-31*::CRE] X
SV2243	*cep-1 (gk138)* I ; *cki-1LOX* II ; *he317* [read-out Blue to red] IV ; *heSi220* [*plin-31*::CRE] X
SV2467	*he317* [read-out Blue to Red] IV ; *daf-3 (ok3610) heSi220* [*plin-31*::CRE] X
SV2468	*cki-1* (*he329*[*cki-1LoxP*]) II ; *he317* [read-out Blue to Red] IV ; *daf-3 (ok3610) heSi220* [*plin-31*::CRE] X
SV2476	*cep-1 (gk138)* I ; *he317* [read-out Blue to red] IV ; *daf-3 (ok3610) heSi220* [*plin-31*::CRE] X
SV2477	*cep-1 (gk138)* I ; *cki-1LOX* II ; *he317* [read-out Blue to red] IV ; *daf-3 (ok3610) heSi220* [*plin-31*::CRE] X
SV2478	*swsn-8 (he273* [loxN exon3])I; *swsn-8* (*he287* [loxN last intron])I ; *he317* [*peft-3*-lox2272NLS::BFP::*let-858* UTRlox2272-NLS::mCherry] IV ; *heSi208* [*Peft-3*::LoxP::NLS *egl-13*::tagBFP2::*tbb-2* UTR::LoxP::NLS *egl-13*::mCherry:: *tbb-2* UTR] V ; *heSi220* [*plin-31*::CRE] X
SV2480	*ubr-5 (he332)* I ; *he317* [read-out Blue to red] IV ; *heSi220* [*plin-31*::CRE] X
SV2481	*ubr-5 (he332)* I ; *cki-1* (*he329* [*cki-1loxP*]) II ; *he317* [read-out Blue to red] IV ; *heSi220* [*plin-31*::CRE] X
SV2482	*cki-1* (*he333* [LoxP intron] II ; he317 [[read-out Blue to red] IV ; *heSi220* [*plin-31*::CRE] X
SV2483	*cki-1* (*he334* [LoxP intron, LoxP synthon] II ; *he317* [read-out Blue to red] IV ; *heSi220* [*plin-31*::CRE] X

Table S2 Overview of used RNA sequences, e.g. primers

Gene name	Primer combination	Sequence	Means	Expected size PCR product wild type (base pairs)	Expected size PCR product mutant (base pairs)
cep-1	OVP669	catcattcgtagccggactg	Detect presence/ absence of *cep-1*	2800	1100
	OVP671	cgttcccgtgaaaacactca			
daf-3	OVP733	cgatttgctgaatttgtgga	Detect presence/ absence of *daf-3*	1315	1015
	OVP734	gatctttcaacgaacctacgc			
cki-1^{lox}	OMG154	CCAGAGAATTGTGTTCCGGAG	Detect presence/ absence of *cki-1^{lox}*	310	280
	OMG155	GTGGAGTTGGTGGCTCTCT			
ubr-5	OVP736	TCCGAATTAGATACAGATTTTTCAATTGTGGAGCAatccGCcGACGGAataagactactgaataaaattatataaaattcttca	Inserting point mutation G>A in *ubr-5* by CRISPR/Cas9	X	X
	OVP737	ATTGTGGAGCAGAGTGCAGA			
ubr-5	OVP716	CACTACGATTCTCTCGGCACA	Confirm point mutation *ubr-5* G>A by sequencing	1100	850
	OVP717	gtagttgatcctaactaagcatgatgg			
ubr-5	OVP717	gtagttgatcctaactaagcatgatgg	Detect presence/ absence of point mutation *ubr-5*	X	963
	OVP735	AGCAatccGCcGACGGAata			
***cki-1^{lox}* new version**	OVP738	ggttctgacagtgagaactt	Inserting new LoxP sites in *cki-1* by CRISPR/Cas9	X	X
	OVP739	ggggtcttccgtggagttgg			
***cki-1^{lox}* new version**	OVP740	/5Sp9/AAGTCGGTCATCTTCTGCTGACGCTTTGTTGGGGTctgaaaatacttcgtataatgtatgctatacgaagttattttaaacttacCTTCCGTGGAGTTGGTGGCT	Repair template for CRISPR/Cas9	X	X
	OVP741	/5Sp9/GTGTTCCGGAGTTCTACAGg			
***cki-1^{lox}* new version**	OMG154	CCAGAGAATTGTGTTCCGGAG	Detect presence/ absence of *cki-1^{lox}* (also for sequencing)	310	340
	OVP742	ACAGCTTGTTTGGAGACAACG			
swsn-8	102	ctgcaaatgtcaactttcatggt	Detect presence/ absence of *swsn-8*	316	282
	103	AAGATGGGCTCTTTTCGCTGG			

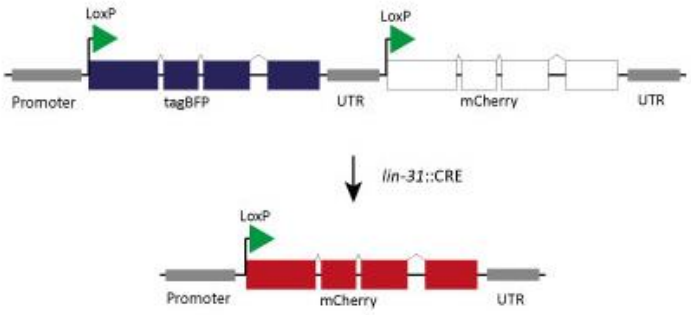

Figure S1 Design of *lin-31::CRE*-dependent BFP-to-mCherry reporter
A promotor drives expression of tagBFP (Blue Fluorescence Protein) flanked by two LoxP sites. A single-copy transgene expressing CRE under the control of the *lin-31* promotor was integrated to induce mCherry specifically in the vulval lineages. The *lin-31* promotor drives expression of Blue Fluorescence Protein (BPF) to mCherry, followed by the untranslated region (UTR). This leads to an easily visible switch from blue-to-red in all (daughter) cells where CRE is expressed, in this case specifically in the vulval lineages.

References

1. Boxem, M. & van den Heuvel, S. lin-35 Rb and cki-1 Cip/Kip cooperate in developmental regulation of G1. *Development* **128**, 4349-4359 (2001).

2. Portegijs, V., Godfrey, M. & van den Heuvel, S. Multiple levels of regulation ensure robust cell cycle exit during C. elegans vulva formation. Manuscript in preparation. (2019)

3. Kipreos, E. T. & van den Heuvel, S. Developmental Control of the Cell Cycle: Insights from Caenorhabditis elegans. *Genetics* **211**, 797-829 (2019).

4. Sherr, C. J. Cancer Cell Cycles. *Science* **274**, 1672-1677 (1996).

5. Galli, M. & van den Heuvel, S. Determination of the cleavage plane in early C. elegans embryos. *Annu. Rev. Genet.* **42**, 389-411 (2008).

6. Umeda, M., Aki, S. S. & Takahashi, N. Gap 2 phase: making the fundamental decision to divide or not. *Curr. Opin. Plant Biol.* **51**, 1-6 (2019).

7. Mohammad, K., Dakik, P., Medkour, Y., Mitrofanova, D. & Titorenko, V. I. Quiescence Entry, Maintenance, and Exit in Adult Stem Cells. *Int J Mol Sci* **20** (2019).

8. Hanahan, D. & Weinberg, R. Hallmarks of Cancer. *Cell* **100**, 646-674 (2000).

9. Hanahan, D. & Weinberg, R. Hallmarks of Cancer: The Next Generation. *Cell* **144**, 646-674 (2011).

10. Hochegger, H., Takeda, S. & Hunt, T. Cyclin-dependent kinases and cell-cycle transitions: does one fit all? *Nat. Rev. Mol. Cell Biol.* **9**, 910-916 (2008).

11. Busino, L., Chiesa, M., Draetta, G. F. & Donzelli, M. Cdc25A phosphatase: combinatorial phosphorylation, ubiquitylation and proteolysis. *Oncogene* **23**, 2050-2056 (2004).

12. Lolli, G. & Johnson, L. N. CAK-Cyclin-dependent Activating Kinase: a key kinase in cell cycle control and a target for drugs? *Cell Cycle* **4**, 572-577 (2005).

13. Bracken, A. P., Ciro, M., Cocito, A. & Helin, K. E2F target genes: unraveling the biology. *Trends Biochem. Sci.* **29**, 409-417 (2004).

14. Weintraub, S. J., Prater, C. A. & Dean, D. C. Retinoblastoma protein switches the E2F site from positive to negative element. *Nature* **358**, 259-261 (1992).

15. Ezhevsky, S. A. *et al*. Hypo-phosphorylation of the retinoblastoma protein (pRb) by cyclin D:Cdk4/6 complexes results in active pRb. *Proc. Natl. Acad. Sci. U. S. A.* **94**, 10699-10704 (1997).

16. Dyson, N. J. & van den Heuvel, S. Conserved functions of the pRB and E2F families. *Nature Reviews Molecular Cell Biology* **9**, 713-724 (2008).

17. Dick, F. A. & Rubin, S. M. Molecular mechanisms underlying RB protein function. *Nat. Rev. Mol. Cell Biol.* **14**, 297-306 (2013).

18. Sherr, C. J. & Roberts, J. M. CDK inhibitors: positive and negative regulators of G1-phase progression. *Genes & development* **13**, 1501-1512 (1999).

19. Ruijtenberg, S. & van den Heuvel, S. G1/S Inhibitors and the SWI/SNF Complex Control Cell-Cycle Exit during Muscle Differentiation. *Cell* **162**, 300-313 (2015).

20. Ruijtenberg, S. & van den Heuvel, S. Coordinating cell proliferation and differentiation: Antagonism between cell cycle regulators and cell type-specific gene expression. *Cell Cycle* **15**, 196-212 (2016).

21. Matushansky, I., Radparvar, F. & Skoultchi, A. I. Reprogramming leukemic cells to terminal differentiation by inhibiting specific cyclin-dependent kinases in G1. *Proc Natl Acad Sci U S A* **97**, 14317-14322 (2000).

22. Mukhopadhyay, D. & Riezman, H. Proteasome-independent functions of ubiquitin in endocytosis and signaling. *Science* **315**, 201-205 (2007).

23. Popovic, D., Vucic, D. & Dikic, I. Ubiquitination in disease pathogenesis and treatment. *Nat. Med.* **20**, 1242-1253 (2014).

24. Schnell, J. D. & Hicke, L. Non-traditional functions of ubiquitin and ubiquitin-binding proteins. *J. Biol. Chem.* **278**, 35857-35860 (2003).

25. Bassermann, F., Eichner, R. & Pagano, M. The ubiquitin proteasome system – Implications for cell cycle control and the targeted treatment of cancer. *Biochim Biophys Acta* **1843** (2014).

26. Metzger, M. B., Hristova, V. A. & Weissman, A. M. HECT and RING finger families of E3 ubiquitin ligases at a glance. *J Cell Sci* **125**, 531-537 (2012).

27. Bashir, T., Dorrello, N. V., Amador, V., Guardavaccaro, D. & Pagano, M. Control of the SCF(Skp2-Cks1) ubiquitin ligase by the APC/C(Cdh1) ubiquitin ligase. *Nature* **428**, 190-193 (2004).

28. Acquaviva, C. & Pines, J. The anaphase-promoting complex/cyclosome: APC/C. *J. Cell. Sci.* **119**, 2401-2404 (2006).

29. Schrock, M. S., Stromberg, B. R., Scarberry, L. & Summers, M. K. APC/C ubiquitin ligase: functions and mechanisms in tumorigenesis. *Semin. Cancer Biol.* **S1044-579X(20)** (2020).

30. Reimann, J. D. *et al*. Emi1 is a mitotic regulator that interacts with Cdc20 and inhibits the anaphase promoting complex. *Cell* **105**, 645-655 (2001).

31. Huang, J. N., Park, I., Ellingson, E., Littlepage, L. E. & Pellman, D. Activity of the APC(Cdh1) form of the anaphase-promoting complex persists until S phase and prevents the premature expression of Cdc20p. *J. Cell Biol.* **154**, 85-94 (2001).

32. Shearer, R. F., Iconomou, M., Watts, C. K. W. & Saunders, D. N. Functional Roles of the E3 Ubiquitin Ligase UBR5 in Cancer. *Mol. Cancer Res.* **13**, 1523-1532 (2015).

33. Wang, Z. *et al*. AKT drives SOX2 overexpression and cancer cell stemness in esophageal cancer by protecting SOX2 from UBR5-mediated degradation. *Oncogene* **38**, 5250-5264 (2019).

34. Tomaic, V. *et al*. Regulation of the human papillomavirus type 18 E6/E6AP ubiquitin ligase complex by the HECT domain-containing protein EDD. *J. Virol.* **85**, 3120-3127 (2011).

35. Albini, S. *et al*. Brahma is required for cell cycle arrest and late muscle gene expression during skeletal myogenesis. *EMBO reports* **16**, 1037-1050 (2015).

36. Joliot, V. *et al*. The SWI/SNF Subunit/Tumor Suppressor BAF47/INI1 Is Essential in Cell Cycle Arrest upon Skeletal Muscle Terminal Differentiation. *PLoS One* **9** (2014).

37. Van der Vaart, A., Godfrey, M., Portegijs, V. & van den Heuvel, S. Dosedependent functions of SWI/SNF BAF in permitting and inhibiting cell proliferation in vivo. *Science Advances* **6** (2020).

38. Mashtalir, N. *et al*. Modular Organization and Assembly of SWI/SNF Family Chromatin Remodeling Complexes. *Cell* **175**, 1272-1288.e20 (2018).

39. Kadoch, C. *et al*. Proteomic and Bioinformatic Analysis of mSWI/SNF (BAF) Complexes Reveals Extensive Roles in Human Malignancy. *Nat Genet* **45**, 592-601 (2013).

40. Wang, X., Haswell, J. R. & Roberts, C. M. W. Molecular Pathways: SWI/SNF (BAF) complexes are frequently mutated in cancer—mechanisms and potential therapeutic insights. *Clin Cancer Res* **20**, 21-27 (2014).

41. Bögershausen, N. & Wollnik, B. Mutational Landscapes and Phenotypic Spectrum of SWI/SNF-Related Intellectual Disability Disorders. *Front Mol Neurosci* **11**, 252 (2018).

42. Zhao, M., Mishra, L. & Deng, C. The role of TGF-β/SMAD4 signaling in cancer. *Int J Biol Sci* **14**, 111-123 (2018).

43. Yang, Y. *et al*. Pokemon (FBI-1) interacts with Smad4 to repress TGF-β-induced transcriptional responses. *Biochim. Biophys. Acta* **1849**, 270-281 (2015).

44. Yamada, S. *et al*. SMAD4 expression predicts local spread and treatment failure in resected pancreatic cancer. *Pancreas* **44**, 660-664 (2015).

45. Weinberg, R. A. in *The biology of cancer* 275-329 (Garland Science, Taylor & Francis Group, United States of America, 2014).

46. Liu, N., Qi, D., Jiang, J., Zhang, J. & Yu, C. Expression pattern of p-Smad2/Smad4 as a predictor of survival in invasive breast ductal carcinoma. *Oncology letters* **19**, 1789-1798 (2020).

47. Lecanda, J. *et al*. TGFbeta prevents proteasomal degradation of the cyclin-dependent kinase inhibitor p27kip1 for cell cycle arrest. *Cell Cycle* **8**, 742-756 (2009).

48. Toufektchan, E. & Toledo, F. The Guardian of the Genome Revisited: p53 Downregulates Genes Required for Telomere Maintenance, DNA Repair, and Centromere Structure. *Cancers (Basel)* **10** (2018).

49. Aubrey, B. J., Kelly, G. L., Janic, A., Herold, M. J. & Strasser, A. How does p53 induce apoptosis and how does this relate to p53-mediated tumour suppression? *Cell death and differentiation* **25**, 104-113 (2018).

50. Ozaki, T. & Nakagawara, A. Role of p53 in Cell Death and Human Cancers. *Cancers (Basel)* **3**, 994-1013 (2011).

51. Fischer, M. Census and evaluation of p53 target genes. *Oncogene* **36**, 3943-3956 (2017).

52. Lewis, E. B. Developmental genetics of Drosophila. *Ann. N. Y. Acad. Sci.* **1038**, 94-97 (2004).

53. Rubin, G. M. Drosophila melanogaster as an experimental organism. *Science* **240**, 1453-1459 (1988).

54. Lewandoski, M. Conditional control of gene expression in the mouse. *Nat. Rev. Genet.* **2**, 743-755 (2001).

55. Brenner, S. The genetics of Caenorhabditis elegans. *Genetics*, 71-94 (1974).

56. Sulston, J. E. & Horvitz, H. R. Post-embryonic cell lineages of the nematode, Caenorhabditis elegans. *Developmental Biology* **56**, 110-156 (1977).

57. Koreth, J. & van den Heuvel, S. Cell-cycle control in Caenorhabditis elegans: how the worm moves from G1 to S. *Oncogene* **24**, 2756-2764 (2005).

58. What Is Cancer? (2015, February 9). Retrieved March 24, 2020, from https://www.cancer.gov/about-cancer/understanding/what-is-cancer

59. Hedgecock, E. M. & White, J. G. Polyploid tissues in the nematode Caenorhabditis elegans. *Dev. Biol.* **107**, 128-133 (1985).

60. Sternberg, P. W. Vulval development. *Wormbook*, 1-28 (2015).

61. Y. Hong, R. Roy & V. Ambros. Developmental regulation of a cyclin-dependent kinase inhibitor controls postembryonic cell cycle progression in Caenorhabditis elegans. *Development* **125**, 3585-3597 (1998).

62. Fukuyama, M., Gendreau, S. B., Derry, W. B. & Rothman, J. H. Essential embryonic roles of the CKI-1 cyclin-dependent kinase inhibitor in cell-cycle exit and morphogenesis in C. elegans. *Developmental Biology* **260**, 273-286 (2003).

63. Schumacher, B., Hofmann, K., Boulton, S. & Gartner, A. The C. elegans homolog of the p53 tumor suppressor is required for DNA damage-induced apoptosis. *Curr. Biol.* **11**, 1722-1727 (2001).

64. Derry, W. B. *et al*. Regulation of developmental rate and germ cell proliferation in Caenorhabditis elegans by the p53 gene network. *Cell Death Differ.* **14**, 662-670 (2007).

65. Ghant, K. Mello Lab CRISPR Protocol. *Mello Lab* (2019).

66. Ji, N. & van Oudenaarden, A. Single molecule fluorescent in situ hybridization (smFISH) of C. elegans worms and embryos. *WormBook*, 1-16 (2012).

67. Stellaris®. (n.d.). Stellaris® RNA FISH. Retrieved August 4, 2020, from https://www.biosearchtech.com/products/rna-fish/

68. Katrukha, E. (2020, April 7). Spots colocalization ComDet (ImageJ). Retrieved August 4, 2020, from https://imagej.net/Spots_colocalization_(ComDet)

69. Liu, F., Pouponnot, C. & Massagué, J. Dual role of the Smad4/DPC4 tumor suppressor in TGFbeta-inducible transcriptional complexes. *Genes Dev.* **11**, 3157-3167 (1997).

70. Kishore, R., & Arnaboldi, V. (2020, March 23). let-526 (gene) - WormBase : Nematode Information Resource. Retrieved August 28, 2020, from https://wormbase.org/species/c_elegans/gene/WBGene00002717#0-9f4-10

71. Artyukhin, A. B., Yim, J. J., Cheong Cheong, M. & Avery, L. Starvation-induced collective behavior in C. elegans. *Sci Rep* **5**, 10647 (2015).

72. Pellegrino, M. W. *et al*. LIN-39 and the EGFR/RAS/MAPK pathway regulate C. elegans vulval morphogenesis via the VAB-23 zinc finger protein. *Development* **138**, 4649-4660 (2011).